Plasma-based dry etching techniques in the silicon integrated circuit technology

by G. S. Oehrlein J. F. Rembetski

Plasma-based dry etching techniques play a major role in the formation of silicon-based integrated circuits. The first part of this paper reviews our understanding of the means for achieving etching directionality and selectivity in reactive etching using glow discharges. Relevant trends in magnetically enhanced rf diode systems, microwave-excited electron cyclotron resonance plasmas, process clustering, real-time process monitoring and control, and computer modeling of glow discharges are discussed in the second part of the paper.

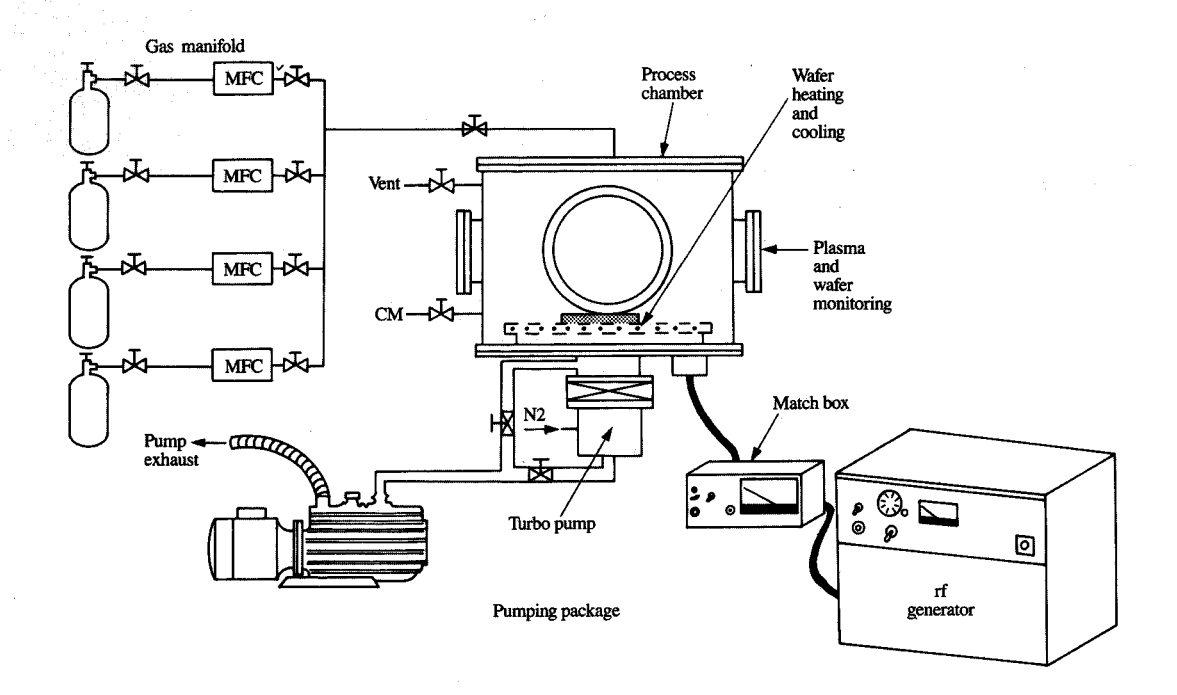
Introduction

The need to accurately reproduce lithographically defined micron- or submicron-scale photoresist patterns in electronic materials during the fabrication of VLSI (very large-scale integration) circuits has been the major driving force behind the introduction of plasma-based anisotropic

etching techniques into integrated circuit manufacturing. Wet etching, which until the beginning of the 1980s was used extensively for pattern transfer, provides high etch selectivity, i.e., the capability to terminate etching precisely at an underlying, chemically different layer. However, the isotropic nature of wet etching results in the loss of critical, lateral dimensions; this is not acceptable in the manufacture of VLSI devices. In addition to being anisotropic, plasma-based etching is compatible with vacuum-based processes such as chemical vapor deposition and molecular beam epitaxy, and is compatible with real-time process diagnostics and control, e.g., endpoint detection.

When a dry etching process is used to transfer a photoresist pattern into an underlayer, the etching process must fulfill a number of requirements: sufficient etch profile control and selectivity with respect to the underlayer and the mask, no significant substrate damage, and, because of productivity requirements, sufficiently high etching rates. The principal difficulty in plasma-based etching is that there is no simple relationship between the process

Copyright 1992 by International Business Machines Corporation. Copying in printed form for private use is permitted without payment of royalty provided that (1) each reproduction is done without alteration and (2) the Journal reference and IBM copyright notice are included on the first page. The title and abstract, but no other portions, of this paper may be copied or distributed royalty free without further permission by computer-based and other information-service systems. Permission to republish any other portion of this paper must be obtained from the Editor.



Components of a generic RIE reactor for etching of electronic materials. The process chamber is evacuated using a turbomolecular pump backed by a mechanical pump. Rf power is supplied to the electrode supporting the wafer by a generator and an automatic matching network (match box). The supply of the reactive gases to the process chamber is controlled with mass flow controllers.

objectives and tool and process variables (e.g., power, pressure, gas mixture, flow). In practice one arrives at satisfactory process results by systematically investigating the response surface of the process; the result is a process "recipe." One of the most important variables in this search is the choice of reactants, also referred to as the "etch chemistry." A great deal of the early work in plasma etching focused on the discovery and optimization of "etch chemistries" [1]. Although this initial work provided many useful industrial etching processes, an understanding of associated mechanisms was typically lacking. Subsequently, the thrust of work in the area of plasma etching was on optimizing the performance of critical etching processes, characterizing and avoiding contamination and damage effects, identifying the important reactive species and measuring their densities, and in general improving our fundamental understanding of plasma-based dry etching. This second phase of the plasma etching work provided insights into the limitations of the initial approaches and resulted in enhanced plasma source configurations and processes which continue to be the subject of ongoing research.

This paper covers the current status of our understanding of some important aspects of plasma-based dry etching, as applied to the silicon integrated circuit technology. The principles underlying the achievement of etch directionality and selectivity in conventional reactive ion etching are reviewed in the first part. The second part focuses on current directions and more exploratory topics that are actively being investigated.

Reactive ion etching

Until now, the most widely utilized dry etching technique has been reactive ion etching (RIE) [2]. The necessary components of a generic reactive ion etching reactor are schematically illustrated in **Figure 1**. The center part of the system is a vacuum chamber which contains an electrode to which rf power (commonly at 13.56 MHz) is capacitively fed using a "match box," i.e., an automatic matching network. The wafer to be etched is placed on the rf-driven electrode. The reactive gases are admitted using mass flow controllers (MFC) from a gas manifold. Halogen-based gases such as CF₄, SF₆, Cl₂, HBr, and mixtures of these gases with O₂, H₂, Ar, and He are

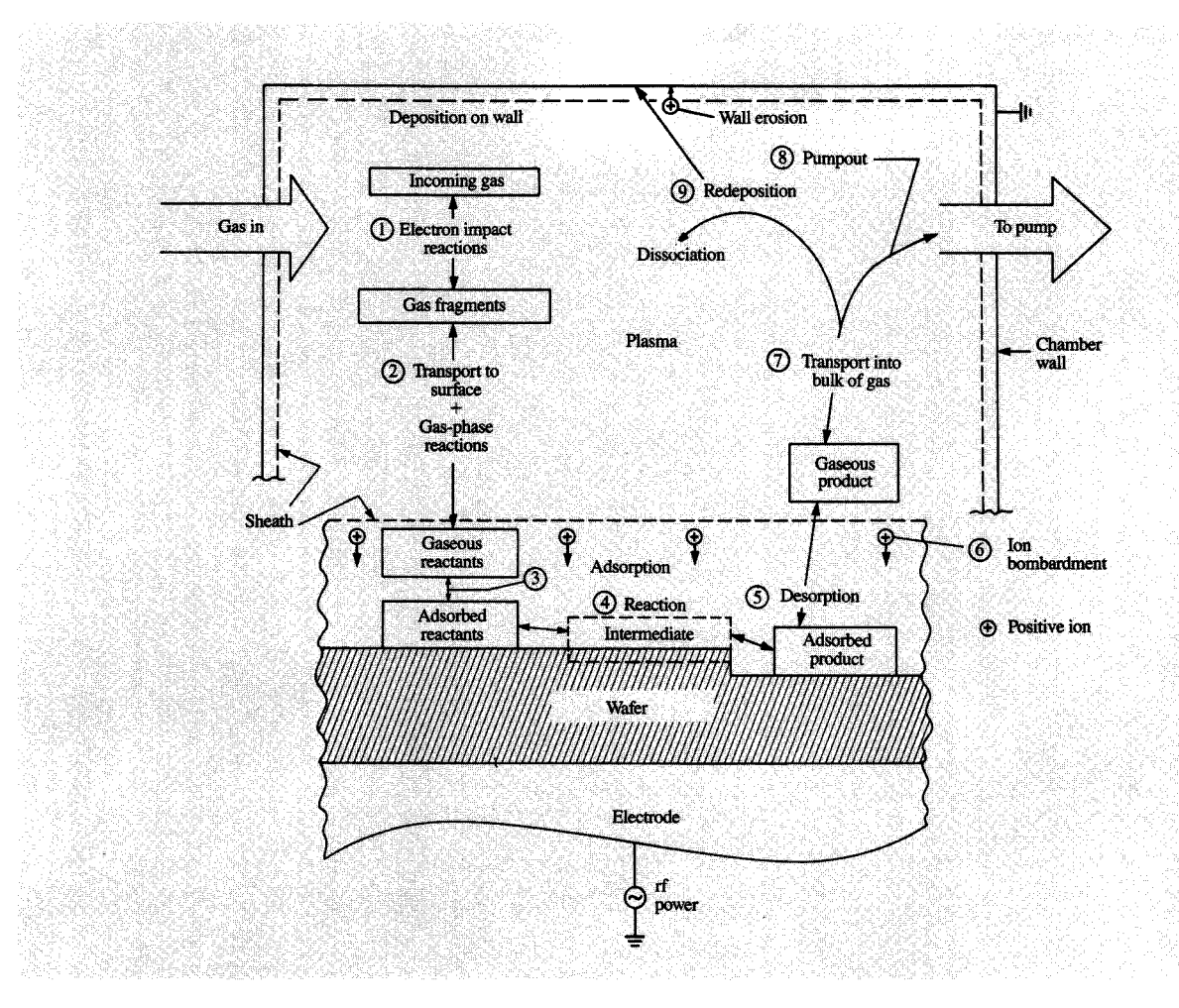


Figure 2

Processes that occur during the plasma etching of a silicon wafer.

utilized for the etching of Si and SiO₂. A typical RIE process is carried out in the pressure range of 10-200 mtorr. The process chamber is evacuated to this pressure range using pumps capable of handling the high flow rates of reactive gases. Reactive species are produced in the following fashion: A large rf voltage (up to $\sim 1 \text{ kV}$) is applied between the substrate electrode and the counter electrode (the latter often being the wall of the chamber), the gas breaks down, and a discharge is established. The gas discharge contains atoms, radicals, positive and negative ions, electrons, and neutral species. Chemical reactions between the discharge-generated atoms and radicals (F, CF₃, CF₂, ...) and the material to be etched (Si) occur at the surface, producing volatile species (SiF₄) which desorb into the gas phase and are pumped out.

In Figure 2 the microscopic processes that occur during plasma-induced etching of a silicon wafer are schematically

shown. The applied rf field serves to accelerate electrons and increase their kinetic energy. The energetic electrons collide with the gas atoms and molecules. Gas atoms and molecules that collide with low-energy electrons are electronically excited; their de-excitation occurs by spontaneous light emission (this process follows quantummechanical selection rules); this is the basis of the "glow" of the discharge. More energetic electrons are capable of dissociating or ionizing gaseous species. The interaction of the atoms and radicals with one another or with the incoming gas increases with pressure, and the resulting gas-phase and surface chemical reactions produce a particular composition of gaseous reactants. This interaction is of particular importance for gas mixtures; e.g., the addition of O, to CF₄ is known to increase the gas-phase density of atomic F by oxidation of CF, radicals [3, 4]. The reactive gas fragments are transported to the

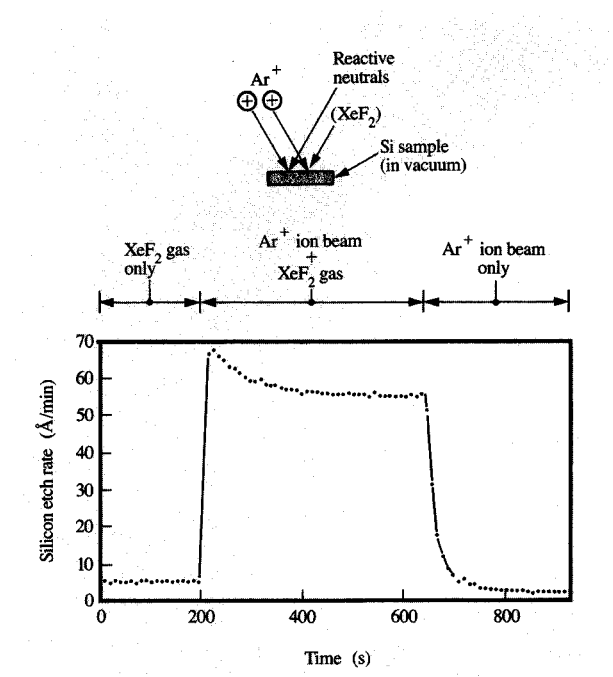
wafer surface where they can be adsorbed. The adsorbed species react to form products with the substrate or desorb from it without reaction. If the product is volatile, it can desorb into the gas phase, where it is transported into the bulk of the discharge. It is then either pumped out or redissociated and involved in further reactions.

Plasma etching itself, without ion bombardment, results in isotropic etching characteristics. Etching directionality in RIE is due to bombardment of the substrate with positive ions, e.g., CF₃⁺ ions in a CF₄ discharge. Ion bombardment enhances or initiates one or all of the fundamental reaction steps occurring at the surface of the substrate and leads to greater vertical than lateral etching rates. Ion bombardment occurs because the discharge causes the substrate electrode to acquire a negative charge, which repels electrons and accelerates positive ions. The negative charge on the electrode is explained by the fact that the mobility of the electrons in the discharge is much greater than that of the ions. Therefore, more electrons initially reach the substrate electrode; because the coupling capacitor prevents any dc current flow, a negative charge is accumulated [2]. The electrode (and the walls) are surrounded with an electron-free positive spacecharge region which is designated as a "sheath." The electric field corresponding to the positive space charge accelerates positive ions entering this region and causes ion bombardment of the electrode. This ion bombardment is not mono-energetic but is characterized by an ion energy distribution function (IEDF) which ranges from zero eV to a maximum value (frequently ~500 eV, corresponding to the full sheath field). The ion energy distribution function often exhibits a complex shape with many peaks which can be explained by the dependence of the IEDF on the ratio of the mean free path to sheath thickness (which varies with pressure) and the number of rf cycles required for an ion to cross the sheath [5, 6].

Since the chamber walls surrounding the plasma are separated from the plasma by a sheath, they can be bombarded with ions of an energy equal to the plasma potential (\approx 20–30 eV in most cases [2]). The walls must therefore be constructed (or covered) with materials compatible with silicon-based electronic materials.

Control of etching profile

Profile requirements in the silicon integrated circuit technology range from near-vertical profiles (e.g., for forming capacitors, trench isolation regions) to sloped sidewalls (e.g., for forming vias) to planarized surfaces (e.g., for forming multilevel interconnections). Plasmabased etching provides a considerable degree of profile control because a) etching characteristics can be altered from being directional to being isotropic; b) the etching selectivity of a material being etched (compared to its etching mask) can be varied continuously by small changes



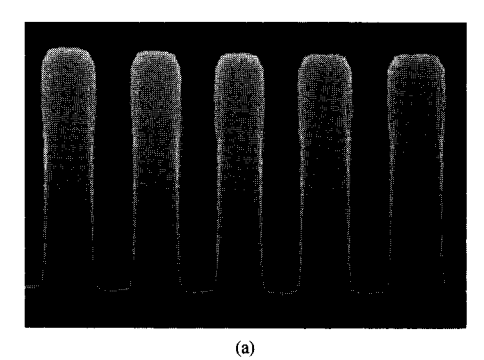
Florina S

Illustration of ion-enhanced etching of silicon using Ar^+ and XeF_2 . The energy of the Ar^+ ions was 450 eV, and the XeF_2 flow rate was 2 \times 10¹⁵ molecules per second. From [7], reproduced with permission.

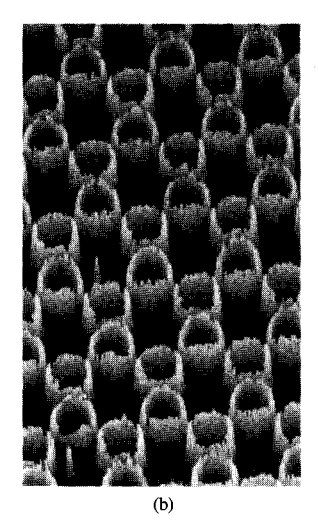
in the "etch chemistry" (thus controllably eroding the mask and introducing a taper into the underlying film); and c) involatile material can be deposited onto sidewalls (not exposed to ion bombardment) and, simultaneously, adjacent surfaces (exposed to ion bombardment) can be etched.

• Ion-enhanced etching

Etching directionality is due to directed energy input into an etching reaction at a surface, and may result from ion, electron, or photon bombardment of that surface. In RIE, etching directionality is achieved by energetic ion bombardment. An important experiment which demonstrated how ion bombardment can enhance an etching reaction was performed by Coburn and Winters and is schematically depicted in Figure 3 [7]. A silicon surface in vacuum was exposed to either a chemical etchant, XeF₂, which spontaneously etches Si at a slow rate, or a flux of 450-eV Ar⁺ ions, or both fluxes simultaneously. Figure 3 shows that the silicon erosion rate obtained for a silicon surface exposed simultaneously to the XeF₂ chemical etchant and the Ar⁺ ion beam is



1 μm



Η 1 μm

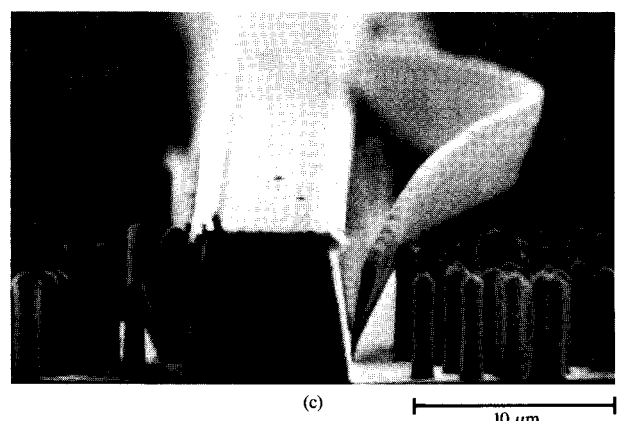


Figure 4

(a) Scanning electron micrograph of a portion of a silicon wafer containing trenches formed by RIE using $HCl/O_2/BCl_3$. Sidewall passivation films can be seen near the top of the trenches. (b) Scanning electron micrograph of a specimen that was etched sufficiently to remove its upper oxide mask and the silicon between its trenches, leaving behind free-standing highly etch-resistant sidewall films. (c) Scanning electron micrograph of a 6- μ m-wide raised line between 48- μ m-wide unmasked silicon regions. The sidewall passivation films appear as wedges on both sides of the line. Numerous small vertical structures can be seen; they are designated as "grass" or "black silicon," and are generally observed in wide, unmasked regions. From [24], reproduced with permission.

much greater than the sum of the etching rates for exposure to the chemical etchant and ion beam separately. Several mechanisms have been proposed to explain such ion-enhanced etching [7, 8]. In the chemically enhanced physical sputtering model [9], the chemically modified surface layer is assumed to have a larger sputtering yield than the unmodified surface. In the damage model, surface damage produced by the ion bombardment is critical [1]. The damaged substrate is assumed to be more reactive than the undamaged material. The most widely accepted model for the fluorine-silicon system appears to be the chemical sputtering model [10], in which ionbombardment-induced collision cascades are assumed to supply energy to the reaction layer and increase the mobility of species in the layer, forming more rapidly volatile products which subsequently desorb. Surface analysis by photoemission, performed on Si wafers initially exposed to XeF, and subsequently bombarded by Ar⁺ ions, is consistent with a model in which the Ar + ion beam aids in the formation of SiF, and volatile SiF₄ from involatile SiF, [11]. There are indications, however, that for different etchant-substrate systems the damage model may be important [12].

The ion beam/chemical etchant synergism can explain the achievement of etching directionality under certain conditions: The bottom of a pattern feature is in the "line of sight" of both chemical species and ions, and the etching rate is high, whereas the sidewall of the feature is exposed only to the chemical species, causing the lateral etch rate (and mask undercut) to be low.

In the etching of integrated circuit structures, a variety of other factors are important and must be considered. For instance, etching of undoped silicon at room temperature in chlorine and bromine plasmas relies on ion bombardment [13, 14]; vertical profiles can be obtained by using, e.g., CL/Ar RIE [15] or HBr RIE [16, 17]. Unfortunately, silicon that is highly doped with group V impurities ($\approx 10^{20}$ cm⁻³) etches spontaneously in a Cl. discharge, and mask undercutting results [15]. This phenomenon is denoted as the "doping effect" [1, 18-20] and is also important for F-based etching. The general observation is that n-type silicon etches more rapidly than does intrinsic silicon, which etches more rapidly than p-type silicon. The observations are qualitatively consistent with a mechanism in which the availability and the transfer of electrons from the semiconductor surface to the chemisorbed halogens increase the rate of etchant reaction with the substrate, although some mechanistic details need still to be established [19, 20]. The fabrication of trenches in the silicon substrate to form capacitor and/or isolation structures requires etching through silicon layers of different doping levels. Since the electronically distinct silicon layers exhibit different lateral etching rates, controlling the profile shape of trenches is difficult. The

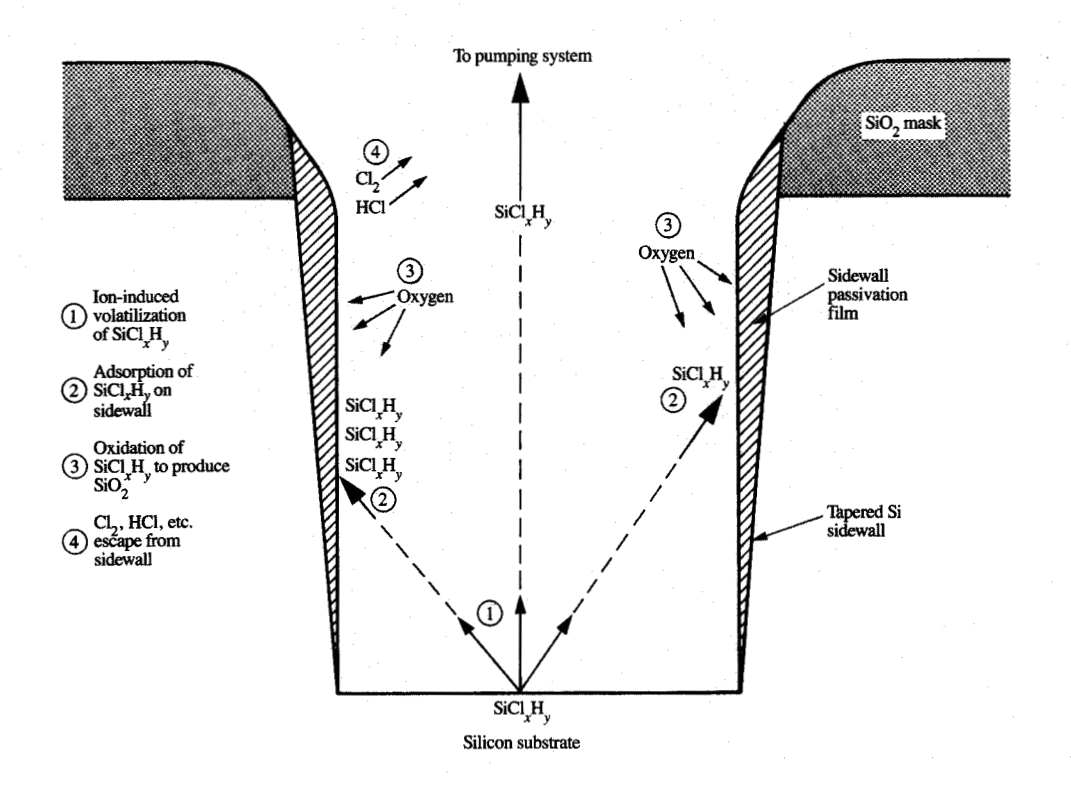


Figure 5

Model of sidewall film formation during the RIE of a trench in a silicon wafer using HCl/O₂/BCl₃. From [24], reproduced with permission.

use of sidewall passivation, discussed next, has helped overcome this problem.

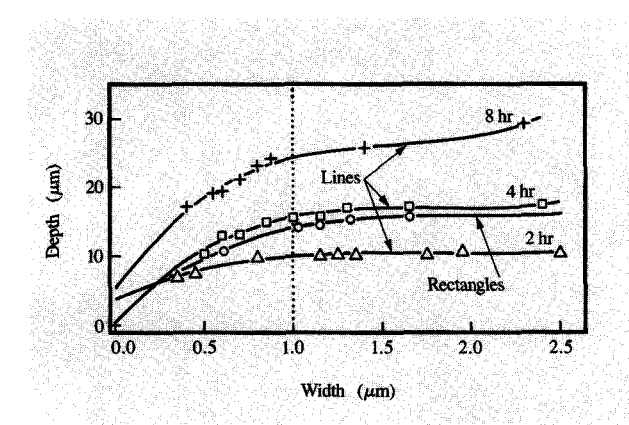
♦ Sidewall passivation

The achievement of etching directionality in reactive ion etching has been found in many instances to result from film-forming processes occurring on the sidewalls of the features being etched [1, 21–23]. These films, known as sidewall passivation layers, slow down or completely stop the lateral attack of etchant species. In sidewall passivation the glow discharge composition is adjusted, e.g., by the addition of O₂ to a Cl₂ plasma, so that film growth occurs preferentially on the sidewalls (not exposed to ion bombardment); film growth is prevented on adjacent horizontal surfaces (exposed to ion bombardment). Sidewall film formation is illustrated in the scanning electron micrographs of Figure 4. Silicon trench profiles formed by HCl/O₂/BCl₂ reactive ion etching are shown in Figure 4(a). The oxide mask used to define the trenches is still in place in the image. The sidewall passivation film is visible as a thin layer near the top of the trenches; it may be isolated by continuing the RIE procedure long enough

to completely erode the oxide mask. After removal of the oxide mask, silicon etches rapidly everywhere, and the etch-resistant sidewall film material becomes visible as the free-standing residue seen in Figure 4(b).

The formation of sidewall passivation films of a finite thickness produces a taper of the silicon sidewall. Figure 4(c) shows a scanning electron micrograph of a 6- μ m-wide silicon line surrounded by 48- μ m-wide unmasked Si regions. The sidewall passivation films have lost adhesion to the sidewalls of the Si line and are wedge-shaped. Because the upper portions of the trench have been exposed to redeposition/oxidation for a longer time, a thicker film exists there. As a result of the sidewall passivation film formation, a taper of \sim 8° was achieved on both sides of the line.

The composition of the sidewall passivation films shown in Figure 4 (RIE using HCl/O₂/BCl₃) has been determined by angle-resolved photoemission and found to be nearly stoichiometric SiO₂, with only small amounts of incorporated Cl [24]. The following mechanism for the formation of the sidewall passivation film was therefore suggested for this "chemistry" (see Figure 5): Ion



Depth and width of lines and rectangles etched into silicon substrates using RIE for various amounts of time. The etching was carried out at 10 mtorr and 13.56 MHz in a load-locked hexode RIE apparatus using an \sim HCl/O₂/BCl₃ gas mixture. The power density was 0.25 W/cm², the initial etching rate was approximately 70 nm/min, and the substrate temperature was 45°C.

bombardment desorbs volatile SiCl, H, products from the horizontal Si surface exposed to the HCl/O,/BCl, discharge. Etch products leaving the Si surface at offnormal angles impinge on the sidewalls of the Si trench and are adsorbed there. Since the mean free path of species in the gas phase is much greater than the feature size (e.g., the mean free path for HCl molecules at 15 mtorr pressure is ~3 mm [25]), the etching products arrive at the sidewall in the state in which they left the Si surface. SiCl, SiCl, SiCl, and Si etching products have been reported [26-30] for the chlorine-based etching of silicon. In particular, the incompletely halogenated Si chlorides such as SiCl and SiCl, appear to be very important for this system [28-30]. These radicals should have a large sticking coefficient on the sidewalls and readily adsorb there. Since the sidewalls are not exposed to ion bombardment, the adsorbed silicon chlorides can reside there for a long time. Oxygen molecules or oxygen atoms formed in the discharge should attack the SiCl radicals adsorbed on the sidewall and produce SiO₂, since such a reaction is highly favored thermodynamically. Volatile Cl., HCl, Cl.O, etc. should be evolved concurrently from the sidewalls. As indicated above, this results in the production on the sidewalls of stoichiometric SiO, films that contain small amounts of Cl and have etching characteristics which are similar to those of the oxide mask.

Sidewall passivation is a rather general phenomenon. For example, the formation of sidewall passivation layers has been observed for the RIE of silicon in fluorine-based [31], chlorine-based [21–23, 32–34], and bromine-based [16, 34–36] plasmas.

Although very satisfactory etch profiles can be produced using this approach, it has many shortcomings. An additional cleaning step is required, since the sidewall passivation layer must be removed prior to further processing. For some processes, so much sidewall passivation is produced that these processes cannot be extended to etching features with a width of less than $0.5 \mu m$, because the passivation layer closes off the feature. Generally, sidewall passivation is based on the formation of involatile material on the sidewalls accomplished by variations in process conditions, e.g., changing the "etch chemistry" by the addition of O, to Cl-based or F-based plasmas, or controlled mask erosion. A basic difficulty with this approach is that the amount of involatile material which is formed depends sensitively on the "pattern factor," i.e., the ratio of unmasked to masked substrate and its spatial variation on the wafer. For an area on the wafer where little substrate is exposed, the process may perform well, but in large unmasked areas difficulties may be seen. This is demonstrated in Figure 4(c), where numerous small Si structures are observed in the wide spaces on both sides of the Si line [for the same process conditions for which very satisfactory trenches are formed in Figure 4(a)]. The formation of these microscopic silicon pillars is well known in trench etching [21]. They are known as "grass" or "black silicon," since a Si surface modified in this fashion appears to be dark when visually inspected. These structures are due to micromasking of silicon in highly selective RIE processes [21, 37–40]. Silicon roughness is introduced if large, unmasked silicon areas are etched using etching "chemistries" with which sidewall passivation is used to achieve etching directionality [24]. Achievement of etching directionality by means of low-temperature etching [41], low-pressure ion-dominated etching using high-density plasmas (to be discussed later), or possibly both shows promise of alleviating these shortcomings.

• Etching of high-aspect-ratio features

The lateral dimensions of features in silicon integrated circuits have continued to decrease as advances have occurred in lithographic and processing capabilities, resulting in the need to increase their vertical dimensions (for example, resulting in the need for thicker metal interconnection lines in order to satisfy electrical conductivity and electromigration requirements, and deeper trenches in order to satisfy capacitance requirements). As shown in **Figure 6**, the RIE of features having submicron openings and a high aspect ratio (ratio of their height to depth) is slower than that of features having larger lateral dimensions and smaller aspect ratios. The depth of trenches in the form of lines and rectangles (i.e.,

long slots) after 2, 4, and 8 hours of RIE is shown as a function of trench width. The trench depth etched after a given amount of time decreases as the trench width decreases, especially for trench widths of less than 1 μ m. This effect increases in importance for longer etching times. The last observation is explained by the general finding made by other investigators [42] that the etching rate is determined by the aspect ratio rather than the trench width, and that the etching rate decreases almost linearly with increasing aspect ratio [42]. Since the aspect ratio of the trench increases with etching time, the incremental etch depth, therefore, falls off with increasing time.

The dependence of etching rate on the aspect ratio is sometimes referred to as "microloading." A slow-down of the etch rate due to microloading, however, is a distinct phenomenon and has a simple origin: The patterned wafer contains a locally higher density of the unmasked substrate, resulting in a local depletion of the etchant and a slow-down of the overall etching rate [43, 44].

The origin of the dependence of the etching rate on aspect ratio is more complex. Several possible mechanisms have been suggested, including distortions of the electric field near the trench, e.g., because of mask charging, which would limit ions from reaching the trench bottom [45, 46], conductance limitations with regard to the supply of reactant to the bottom of the trench [47], and the scattering of ions in the sheath above the wafer [48]. The behavior of the aspect-ratio-dependent etching rate as a function of pressure provides some important indications regarding the mechanism(s) underlying this phenomenon [49]. For plasma etching at 2 torr and reactive ion etching at 50 mtorr, a strong dependence of the etching rate on trench diameter has been found [49]. On the other hand, for microwave-based etching at 3 mtorr, the etching rate has not been found to depend on trench diameter [49]. Similar observations have been made by another group and explained in terms of the pressure dependence of the probability for ion scattering in the sheath [48]. Ion scattering in the sheath increases the mean impact angle width [50]. As the depth of the narrow feature increases, the solid acceptance angle for ions decreases and, for processes strongly dependent on ion-induced etching, the etch rate will decrease.

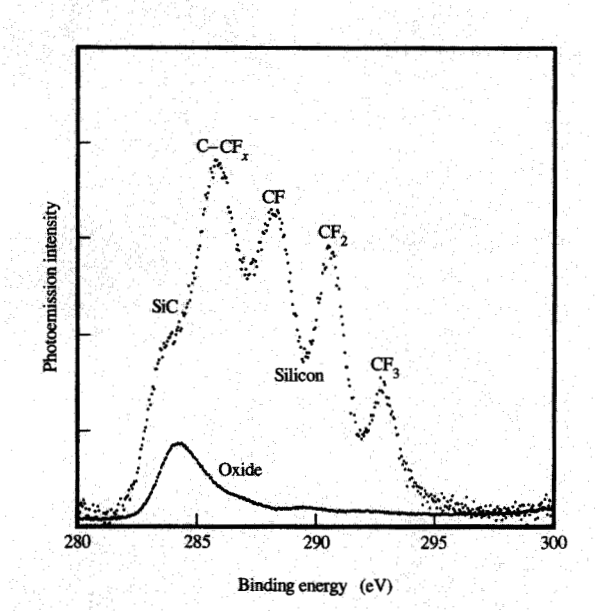
At this time, it appears that the only solution for etch applications for which aspect-ratio-dependent etching is a problem is low-pressure etching [49].

Etch selectivity

The ability to achieve large etch rate ratios (ERR) between chemically different materials is the crucial advantage of reactive etching techniques over purely physical sputtering techniques. Etch selectivity of a film being patterned is required with respect to the etch mask and the substrate. Etch selectivity of a material A over a material B in reactive ion etching is due to rate differences in the elementary steps taking place at the surfaces of these materials, e.g., differences in adsorption, reaction, or etch product desorption. The mechanism underlying the achievement of SiO₂-to-Si RIE selectivity is now discussed.

SiO₂-to-Si etch selectivity

Selective etching of SiO₂ over Si is accomplished using fluorine-deficient fluorocarbon plasmas based on CHF₂, CF₄/H₂, or related gas mixtures [51–53]. In the gas phase of these discharges, a multitude of different species exist simultaneously, and these species impinge on the surface of the substrate. As a result several processes occur concurrently at the substrate surface; e.g., for a CF₄/H₂ plasma, fluorine-induced etching competes with CF₂radical-initiated fluorocarbon film growth. Advantage is taken of these processes to achieve etch selectivity in the following manner: Processing conditions are chosen so that etching and deposition in fluorine-deficient CF₄/H₂ or CHF₂ plasmas are nearly balanced for the first material. For the same process conditions, this balance can be tilted to either etching or deposition for a second material. Fluorocarbon deposition occurs for suitable discharge conditions on the Si surface and slows down the Si etching rate [54]. For the same discharge conditions, the SiO₂ surface remains free of deposited fluorocarbon. These differences in carbon contamination on CF₄/H₂-plasma-etched Si and SiO₂ surfaces are demonstrated by the X-ray-induced carbon 1s photoemission spectra in Figure 7. The photoemission spectrum obtained with an etched Si surface exhibits a high intensity of characteristic C-CF, CF, CF, and CF, groups because of the existence of a fluorocarbon film. The photoemission spectrum obtained with an etched SiO, surface exhibits only a very low intensity of fluorocarbonrelated groups and primarily C-C and Si-C-type bonding. The fluorocarbon film prevents the fluorination of the silicon which is necessary to sustain its etching. This has been shown in a study of the degree of Si fluorination beneath the fluorocarbon film, which verified that with increasing film thickness the degree of Si fluorination dropped [54]. Hydrogen must be added to fluorocarbon plasmas to initiate fluorocarbon deposition on Si, since atomic hydrogen reacts 1) with atomic F to form HF, thus reducing Si and fluorocarbon etching, and 2) with CF₃ radicals to form HF and CF₂, thus increasing the density of CF, fluorocarbon film precursors [56, 57]. Etching selectivity for SiO₂/Si is a consequence of the presence of oxygen in the SiO₂. During RIE of SiO₂, oxygen is continuously produced at the etching surface. The oxygen can react with the fluorocarbon film precursors to form volatile CO, CO₂, and COF₂, preventing the



Carbon 1s photoemission spectra of SiO_2 and Si surfaces after RIE using $CF_4/40\%H_2$ at 25 mtorr to selectively etch the SiO_2 . The selective formation of an \sim 3-nm-thick fluorocarbon film on the Si prevented its etching. From [55], reprinted by permission of the publisher, The Electrochemical Society, Inc.

formation of an etch-inhibiting fluorocarbon film on the SiO₂ surface. Oxide etching can therefore continue.

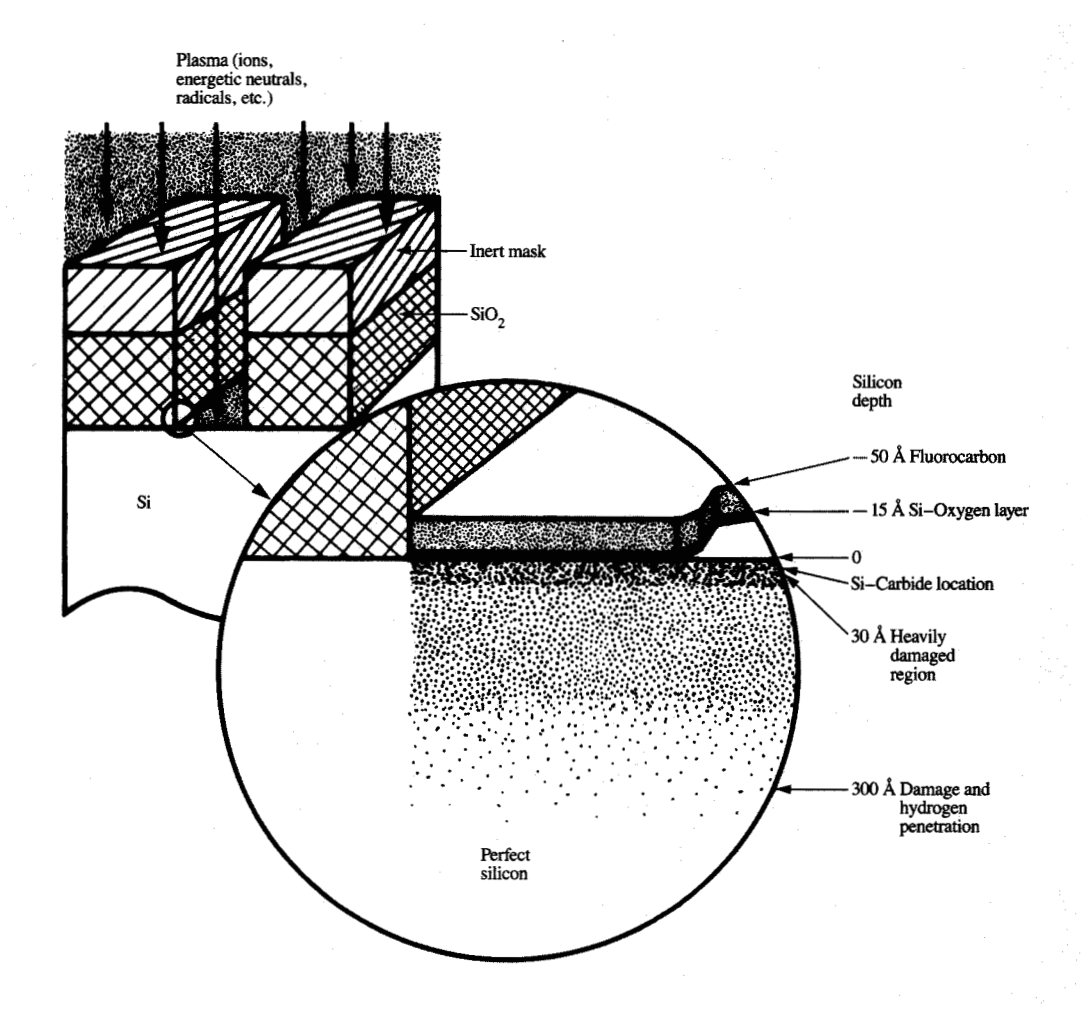
Damage and contamination effects

The achievement of etch directionality and selectivity is associated with undesirable effects of the plasma on the substrate. Etch anisotropy is due to bombardment by energetic ions. In RIE the ion energy cannot be controlled independently of the production of the plasma; i.e., increasing the rf power increases both plasma density and ion energy. Ion energies may be as high as 300 to 700 eV and, at typical fluence rates of $\sim 10^{15}$ ions/cm²s, bombardment damage can occur. Displacement damage can alter the near-surface region of the material which is being etched (or exposed to the plasma) and change its electrical properties. The subject of damage due to ion etching has been reviewed [58]. Substrate contamination is another important concern. As discussed in the previous section, selective etching is often due to the deposition of etch-inhibiting films. Such films can remain on the substrate after completion of the etching and interfere with subsequent device processing.

The near-surface damage and contamination effects of a Si surface introduced by selective oxide removal using

CF₄/H₂ or CHF₃ have been studied by a great number of investigators and are well established [59-65]. The schematic shown in Figure 8 [66] depicts a Si surface after selective oxide etching using CF₄/40%H₂. After RIE, the Si surface is covered with a continuous fluorocarbon film that is roughly 35 Å thick and contains very little Si. A thin SiO, layer is present beneath the film; it is not residual SiO, from the selective etching process, but is formed after air exposure of the plasma-etched Si specimen. A region of heavily disordered Si in which silicon-carbon bonding is present [67] extends ~30 Å below the Si surface. A region of less heavily damaged Si is observed to extend beyond 300 Å from the Si surface, and this region contains a high concentration of hydrogen, as shown by nuclear reaction profiling. By substituting deuterium for hydrogen in RIE, and by using secondary ion mass spectrometry (SIMS) to detect D in Si with low background concentration, an unexpectedly large penetration depth of D into Si has been observed. For example, D at concentrations of 10¹⁷ atoms/cm³ has been detected at a Si depth of more than 200 nm from the surface after one minute of plasma exposure. By using transmission electron microscopy, hydrogen-induced extended defects have been observed in the first 300 Å of Si [66, 68, 69]. Such surface modifications necessitate the use of surface-cleaning/damage-removal processes which must be performed prior to further device processing. The necessary cleaning/damage-removal treatments greatly complicate the processing; improved etching tools and procedures which minimize contamination and damage effects are required for increased productivity.

Recently it has been shown that the chemistry of many discharges is prone to the formation of negatively charged particles [70-73]. The particles become suspended at the plasma/sheath boundary just above the wafer surface. For some plasma conditions, the presence of 0.2-μm-diameter particles at densities greater than 10⁷ cm⁻³ has been inferred from laser-light-scattering experiments [71]. The particles remain in the negative charge state for most or all of the total etching time and grow in size while floating above the wafer, forming three-dimensional structures related to the topography of the electrode; their presence can be observed using laser light scattering [71]. Figure 9 shows laser light scattering from rings of such particles around the outside edge of Si wafers and from domes of such particles over the centers of the wafers during operation of an Ar plasma [71]. Although such particles remain negatively charged and can float above the wafers for a considerable time, neutralization and deposition onto the wafer surfaces can take place, in particular at the end of the process [70]. There appears to be a good correlation between yield loss and particle counts [70]. Etching gas mixtures with a low propensity for particle formation (e.g., those containing fluorine) produce fewer particles than do



Near-surface modifications of a Si substrate after selective oxide RIE using CF₄/40%H₂ or CHF₃. From [66], reproduced with permission.

those containing chlorine [70]. In addition, strict adherence to tool-cleaning schedules and plasma operation at low pressure are expected to alleviate this problem.

Recent developments and current trends

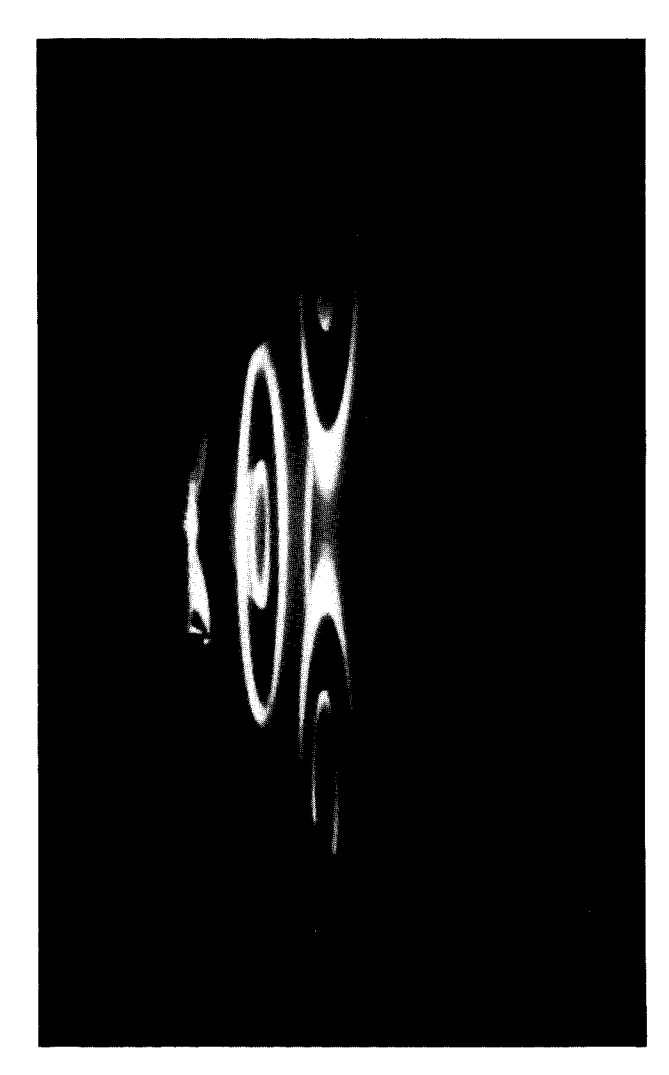
Low-pressure single-wafer reactors

The etching rates possible in RIE are low, and throughput considerations dictate multiwafer processing, e.g., up to 24 six-inch Si wafers for commercial systems. Increases in semiconductor wafer size, up to a diameter of eight inches currently, and the demand for greater process automation (e.g., microprocessor-controlled cassette-to-cassette loading/unloading) and improved process control (e.g., individual endpoint detection), have established single-

wafer-etching equipment as the standard for many applications. To achieve adequate throughput, high etching rates ($\approx 0.5-1~\mu \text{m/min}$) are required for single-wafer reactors. A high reactive-species generation rate is a prerequisite of a high etching rate and high throughput. The generation rate R_i of the *i*th reactive species in a glow discharge by electron impact can be expressed [74] as

$$R_{i} = n_{e} N \int_{0}^{\infty} \sqrt{\frac{\varepsilon}{2m_{e}}} \, \sigma_{i}(\varepsilon) f(\varepsilon) \, d\varepsilon, \qquad (1)$$

where n_e is the electron number density, N is the neutral gas number density, ε is the electron energy, $f(\varepsilon)$ is the electron energy distribution, m_e is the electron mass, and $\sigma_i(\varepsilon)$ is the cross section for the *i*th process (dissociation,



Elfalmase

Photograph of laser light scattering from particles suspended above a graphite electrode covered by three 82-mm-diameter Si wafers during exposure to an Ar plasma. The particles were negatively charged and suspended at the plasma/sheath boundary. The photograph shows that the particles were organized in three-dimensional structures as rings of particles around the outside edge of the Si wafers and as domes of particles over the centers of the wafers. From [71], reproduced with permission.

ionization, etc.). The cross section $\sigma_i(\varepsilon)$ shows a threshold as a function of energy, e.g., the ionization potential in the case of ionization, below which it is zero. Increases in either the number density $n_{\rm e}, N$, or the mean electron energy are expected to cause a larger generation rate of reactive species. The initial approach for single-wafer reactors was to operate at a high gas pressure (≈ 1 torr and greater) and use a small interelectrode gap (less than 1 cm) and high rf input power, thus achieving high generation rates of the reactive species and high etching rates. High-

pressure single-wafer reactors are characterized by a low ion-to-neutral-particle ratio and fairly low energy of the bombarding ions (because of ion-neutral-particle collisions in the sheath). Directional etching in these systems is due to sidewall passivation.

Directional etching of materials for which sidewall passivation is difficult to achieve, or etching of materials requiring a significant sputtering component (e.g., involatile CuCl_{x} removal for etching of Al–Cu films, etching of SiO_{2}) is preferably performed at low pressure. Two important low-pressure single-wafer etching processes are magnetically enhanced reactive ion etching (MERIE) and electron cyclotron resonance (ECR) etching.

• Magnetically enhanced reactive ion etching In magnetically enhanced reactive ion etching, the combination of magnetic field lines parallel to the cathode surface (produced either by external electromagnets or permanent magnets) and electric field lines (due to the cathode dc bias) confines electrons on cycloidal trajectories near the cathode [75]. The resulting trajectory of an electron produced near a wafer is shown in Figure 10. The associated confinement reduces electron losses to the walls of the system and increases the frequency of electron-neutral collisions compared to that in a conventional RIE reactor. The ion/neutral ratio can thus be increased by a factor of about 50 in RIE [75]. Because the magnetic confinement reduces the mobility of electrons toward the cathode, the self-bias voltage produced in MERIE systems is lower than in comparable RIE systems. Although plasma production and wafer bias are not decoupled, the self-bias voltage at the powered electrode is reduced to values approaching 100 V and results in reduced substrate damage [76].

A comparatively large flux of low-energy ions is produced in MERIE systems at low pressure. Anisotropic etching is easier to achieve at a low pressure, since both a higher ion-to-neutral flux ratio and the reduced probability of ion-neutral collisions in the sheath result in less bowing or barreling (rounded sidewall shapes) [77].

Electron cyclotron resonance (ECR) plasmas

In electron cyclotron resonance (ECR) etching, a gas
discharge is produced by microwave excitation (commonly
2.45 GHz) in the presence of a magnetic field [78]. The
Lorentz force causes the electrons to circulate around the
magnetic field lines with the cyclotron frequency

$$\omega_{ce} = \frac{eB}{m_e},\tag{2}$$

where e is the electronic charge, B is the magnetic flux, and m_a is the electron mass. At a magnetic field strength of

875 gauss, the cyclotron frequency is calculated to be 2.45 GHz, the microwave frequency allocated for industrial use. For this condition, the electrons are continuously accelerated by the electric field and acquire large velocities, and the energy coupling becomes resonant. Ultimately, an electron collides with a gas atom or molecule and because of its large kinetic energy, ionizes or dissociates the gas species. Because of resonant electron heating, ECR-based discharges are characterized by a high degree (in the percent range relative to 10⁻⁶ for RIE) [78] of ionization and dissociation, facilitating the achievement of high plasma densities at low pressures.

In Figure 11, one of the possible configurations [79] of a plasma etching (or deposition) system containing an ECR plasma source is shown. The ECR source is mounted above the processing chamber. Microwave power is coupled via a waveguide through a dielectric window into the ECR source region. This space is surrounded by coils providing a magnetic field **B** of ~1 kgauss. The magnetic field decreases as a function of distance from the coils. At

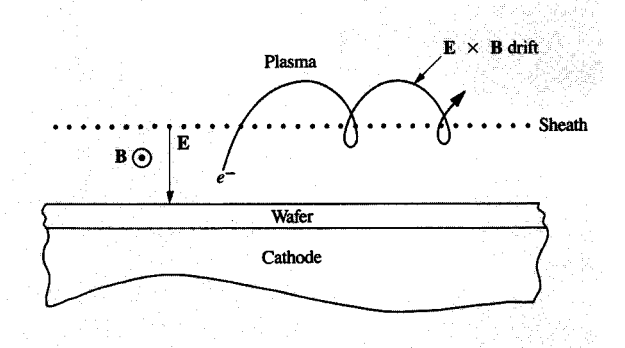
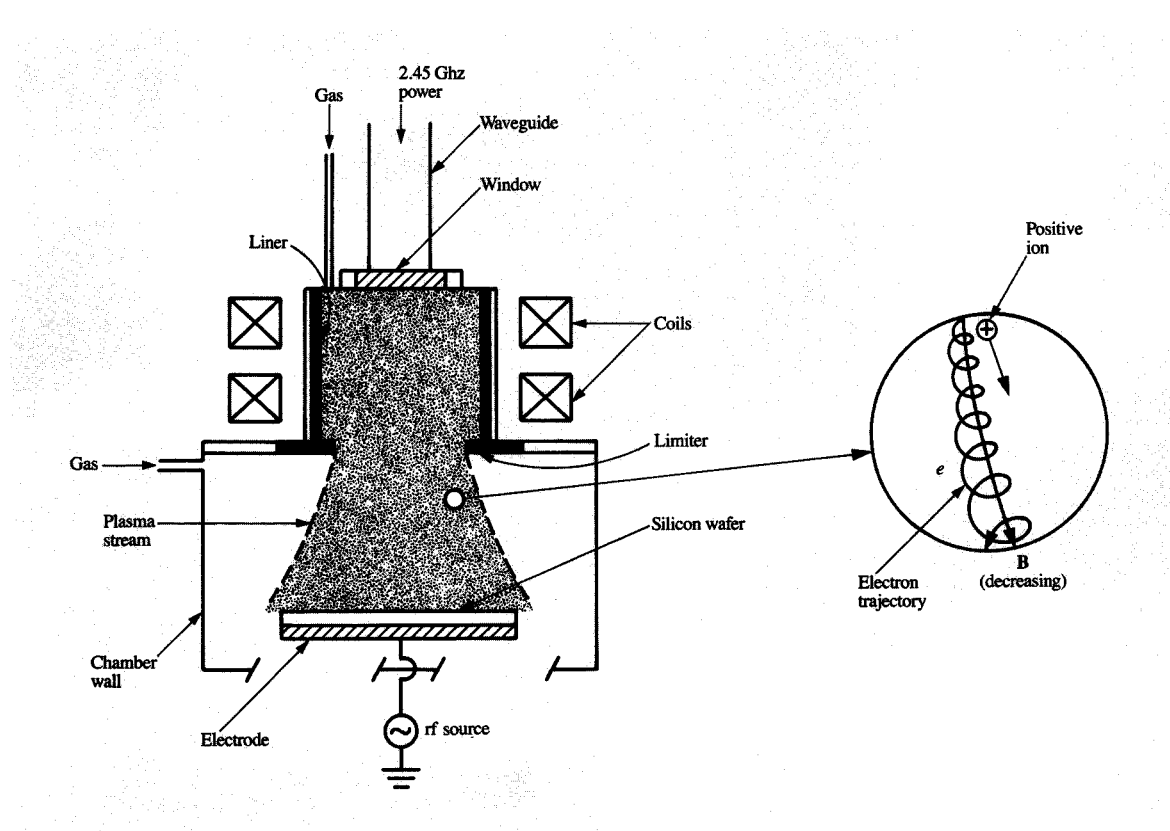


Figure 10

Magnetically enhanced reactive ion etching reactor. The combined action of electric and magnetic fields forces the electrons on cycloidal paths near the plasma/sheath boundary. The resulting confinement of the electrons to a region close to the wafer results in enhanced dissociation and ionization rates, and facilitates more rapid etching than in the absence of the magnetic field.



Floure 11

Schematic diagram of a plasma etching system containing an ECR plasma source. The plasma is formed in a tube surrounded by two current-carrying coils that produce a magnetic field inside the tube, and diffuses out of the tube into the process chamber. The silicon wafer can be rf- or dc-biased.

certain locations within the ECR source, the field is 875 gauss, the ECR condition is fulfilled, and the microwave energy is resonantly absorbed by the electrons. Electrons and ions diffuse by ambipolar diffusion out of the resonance region into the lower process chamber where a Si wafer is located. The wafer can be rf- or dc-biased to control the energy of impinging ions.

The microwave resonance absorption phenomenon as a means of coupling energy to electrons is effective only at operating pressures below ~10 mtorr. Above this pressure, electron-gas collisions become too numerous to allow the phenomenon to be established.

From a practical viewpoint, low-pressure operation in ECR (and MERIE) plasma(s) greatly increases the demands on the pumping equipment and wafer cooling compared to what is required for RIE. Since etching rates acceptable for manufacturing environments require high gas flows, a relatively large pumping system must be employed in order to achieve ECR operating pressures. Back-side helium cooling of the wafer, employing either a mechanical clamp or an electrostatic chuck, is necessary for control of the wafer temperature and the etching process. On the other hand, ECR plasma processing provides the advantage of true decoupling of plasma production from wafer biasing, resulting in less dry etching damage than is encountered in RIE [80].

There is considerable effort underway with respect to the designing and testing of novel high-plasma-density sources based on different physical means for coupling electrical energy to electron motion at low pressure, e.g., the excitation of helicon waves [81]. These developments show promise of being able to overcome some of the limitations inherent in the ECR approach.

• Process clustering

Multilevel metallization plays a key role in high-density integrated circuits. The metal films used for this purpose are often deposited in multichamber (or cluster) systems in order to ensure control of interface and film properties and low levels of contamination. Such a multichamber system approach is useful for dry etching as well. Illustratively, Figure 12 depicts the use of a multichamber tool to carry out several dry processing steps.* The system contains four etching chambers and a vacuum load-lock. All five chambers are connected by a central-wafer handler which moves the wafers from one chamber to the next in vacuum. The advantages of this approach are that no air exposure of the wafers between the etching steps is required, and that no cross-contamination of the different processes that are carried out occurs; such crosscontamination would occur if only a single chamber were

The process simplification which results from vacuum transfer increases throughput and minimizes microroughening, post-etch corrosion, and other deleterious effects, ultimately increasing yield. This approach is attractive for most process sequences in which several consecutive etching steps must be carried out. Alternatively, the same etching processes may be run concurrently in the different chambers of the apparatus. Since the etching chambers share the load-lock and central wafer handler, clean-room space is conserved.

The clustering of dry etching processes with chemical vapor deposition processes is also of interest. This facilitates the implementation of sequential deposition/etching processes which, for instance, are required in the formation of trench collars and lightly doped drain (LDD) spacers.

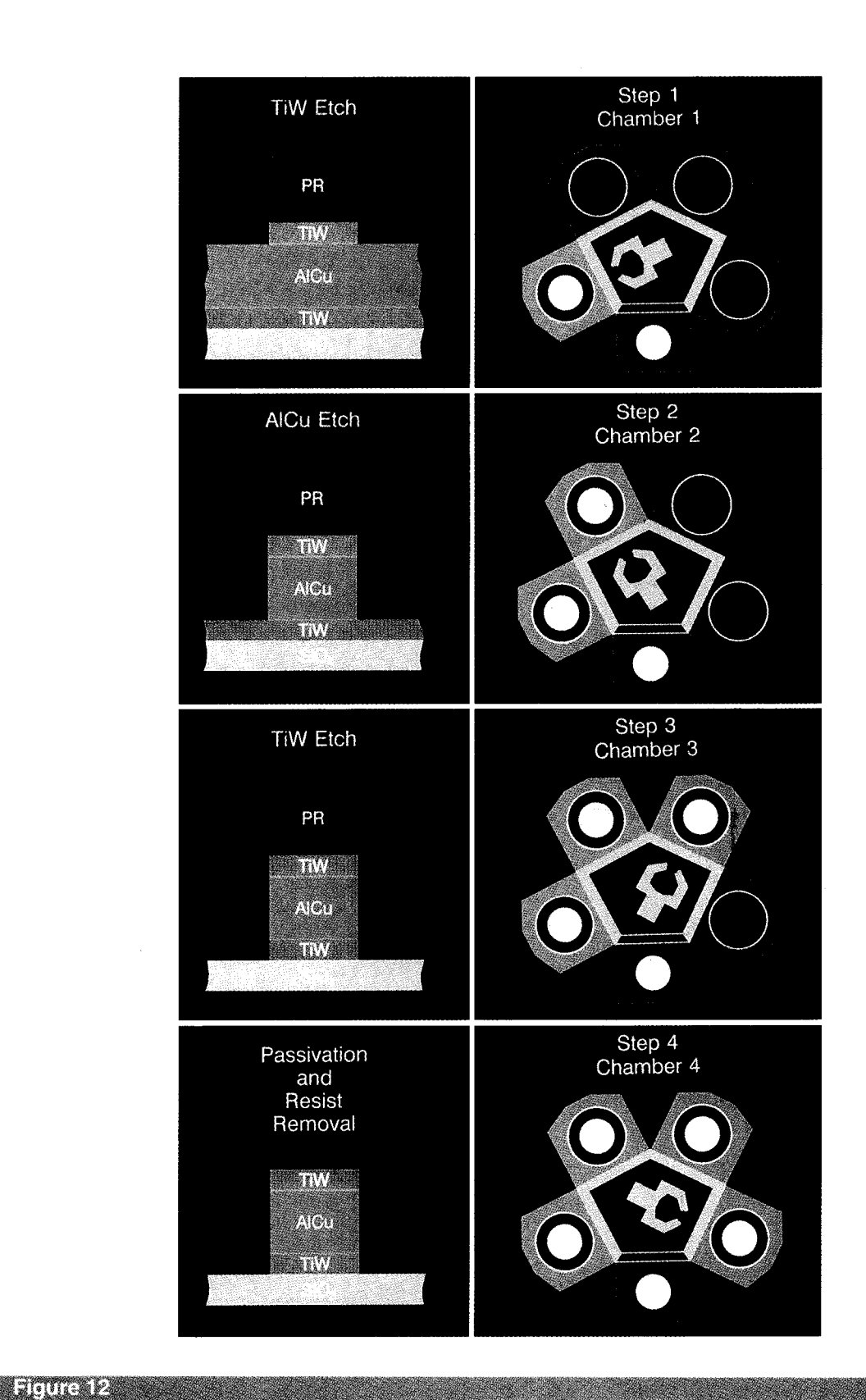
• Real-time monitoring and control

The value of partially processed Si wafers is increasing because of the increase in processing complexity and the use of larger Si wafers. This justifies investing in in-process monitoring equipment which can detect equipment/process malfunctioning. In-process control of the etching process in integrated circuit manufacturing is currently limited to endpoint detection. Optical emission spectroscopy (OES), neutral mass spectrometry using a residual gas analyzer (RGA), or thin-film laser interferometry are conventionally used for endpoint detection. In OES, a strong emission line of a reactant or an etchant product is monitored, and the intensity change associated with completion of the etching of one layer is used to signal the etching endpoint.

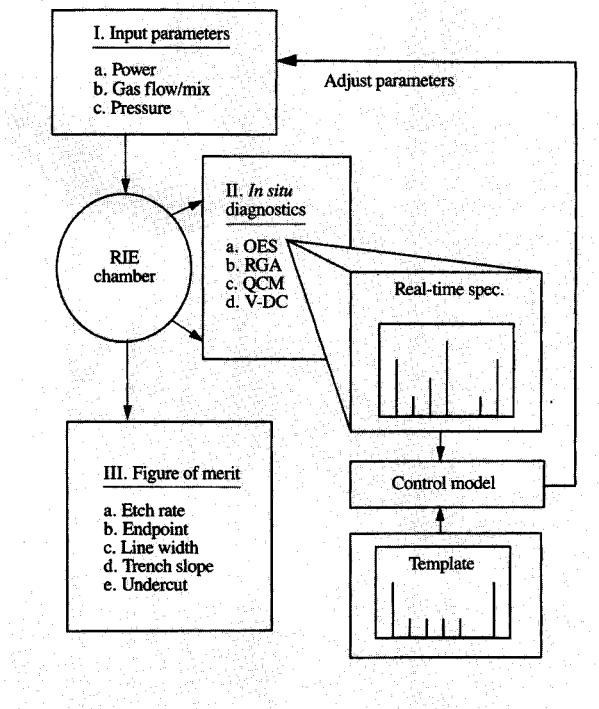
This approach discards a great deal of potentially useful information, since OES is able to provide information on a variety of plasma species. For example, Banks et al. [83] have shown that the achievement of isotropic or directional etching profiles in photoresist layers can be correlated respectively with the optical emission intensities of the O atoms or O_2^+ ions that are present. The O/O_2^+ ratio can be controlled by changing the rf power and pressure of the O_2 plasma. Comprehensive in-process monitoring of the etching process is also desirable, since one of the complications encountered in plasma etching is that the response surface drifts as a function of system usage, e.g., because of the deposition of process-related films on the chamber walls.

used. Since the wafer is not exposed to atmosphere during transport from one chamber to the next, the number of etching initiation steps required (native oxide removal treatments to prevent microroughening) can be minimized. For AlCu etching, post-etch corrosion is a serious problem, requiring a post-RIE passivation treatment [82]. AlCu passivation is achieved in the system during the final in situ photoresist stripping process.

^{*}Manufactured by the Drytek Corporation, a unit of the General Signals Corporation, Wilmington, MA 01887.



Illustrative dry processing of a TiW-AlCu-TiW composite film in a four-chamber cluster system. (Courtesy of the Drytek Corporation, a unit of the General Signals Corporation, Wilmington, MA 01887.)



System for RIE with in-process control. During operation, optical emission spectra (OES) data, residual gas analysis (RGA) data, quartz-crystal microbalance (QCM) data, and $V_{\rm dc}$ data are continuously acquired and compared to a set of prescribed values. If deviations occur, a control model is used to adjust system parameters or stop the processing and warn the system operator. From [84], reproduced with permission.

In Figure 13, a prototypical system used for RIE with in-process control is shown schematically [84]. The controllable input parameters are rf power, gas flow, and pressure. A discharge is established using prescribed values of parameters. Optical emission spectroscopy, residual gas analysis, etc. are used to monitor the discharge in real time and provide information on a broad variety of identified plasma species. Initially, "training runs" are used to establish a correlation between the result of the diagnostic measurements and the figures of merit (etch profile, etch selectivity with respect to mask and underlayer, etc.) of the process. During an actual run, the results of the in situ diagnostics are used to calculate the figures of merit expected for that run. There are several levels of in-process control: 1) disaster recovery—e.g., a leak is detected and the system is shut down; 2) preventive maintenance-e.g., a signal indicating the necessity for chamber cleaning is detected and the operator is informed; and 3) adaptive process control [84]. In adaptive process

control, a control algorithm is used to either adjust the input parameters in real time to obtain desirable figures of merit or stop the processing.

• Modeling of plasma etching

Computer models of various aspects of plasma-based etching processes have the potential to dramatically enhance our efficiency to design and optimize etching systems and improve our utilization of etching processes. For example, two-dimensional plasma source and system modeling should be useful in improving etch uniformity and in the design of large reactors. A fully predictive model of the plasma etching process requires, in addition to treatment of both the discharge physics and chemistry, which are coupled [85], the simulation of relevant surface processes. Such a model is impractical at this time because of a) its excessive computing power requirements; b) a lack of knowledge of many of the input parameters for some of the complex gas mixtures used in etching (electron impact cross sections, gas-phase and surface chemical rate coefficients, etc.); and c) a lack of mechanistic insights regarding, e.g., details of plasma-surface interactions. A variety of simpler models which treat part of the overall problem have therefore emerged. Depending on the characteristic length inherent in a particular model, system scale models, boundary-layer scale models, feature scale models, and atomistic scale models relevant to etching processes currently exist.

In system scale models, use is made of input parameters such as reactor geometry, rf power, gas flow, and pressure; electron density and energy distribution, radical and ion densities, their energies, etc. are obtained as a function of position and time. There are four basic types of such models: equivalent circuit models [86], analytic plasma models with certain simplifying assumptions, e.g., assuming a Maxwellian electron energy distribution [87, 88], fluid models for intermediate pressure discharges [85, 89-91], and kinetic models for low-pressure discharges [92, 93]. Although review of the large amount of published work on this subject is beyond the scope of this paper, some results obtained by Vender and Boswell [93] are presented in Figure 14 to illustrate what can currently be achieved. The evolution of the electric field in the space between the two electrodes of a symmetric diode system is shown as a function of time, as obtained by a particle-incell simulation of the plasma [93]. The results of the simulation show that the electric field variation is restricted to the plasma sheaths, and that the electric field vanishes in the bulk of the discharge.

In boundary-layer models, account is taken of physical processes in the sheath, e.g., ion scattering. The angle and energy data of impinging ions obtained are used as input data for feature scale models in which the profile evolution of features is simulated [33, 94, 95]. String advance

algorithms are used to obtain the etching profile as a function of time from the initial profile and the angle and energy data of impinging ions by assuming angle-dependent etching rates and redeposition [33, 94, 95]. Such modeling has probably had the most direct impact on the integrated circuit technology, e.g., by enabling the rapid evaluation of the effect of line proximity and trench aspect ratio on the profile shape.

In atomic scale models, the interactions of ions, radicals, and molecules with the substrate are taken into account. For example, molecular-dynamics simulations have been used to analyze the interaction of low-energy (40 eV to 1 keV) Ar⁺ ions with a (100) Cu surface (previously examined experimentally) [96]. The analysis shows promise of providing important, relevant insights on energy deposition, trapping of ionic species in the first few layers of the substrate, ion-induced chemical reactions, and other aspects of ion-enhanced etching.

Concluding remarks

Plasma-based etching of electronic materials has rapidly evolved from a process involving the use of converted sputter-deposition systems [97] to one involving the use of multichamber systems, high-density plasma sources, inprocess monitoring, etc. The volume of work in this area has increased similarly, with some 400 to 500 relevant papers appearing in the literature in 1991. Despite the large effort, plasma-based processing (etching and deposition) continues to be characterized primarily by "recipes" or "chemistries." More understanding will be needed of the mechanisms that underlie the processes used and their implications regarding yield if the rapid pace of advance in this area is to continue.

References

- 1. D. L. Flamm and V. M. Donnelly, Plasma Chem. Plasma Process. 1, 317 (1981).
- 2. J. W. Coburn, Plasma Etching and Reactive Ion Etching, American Vacuum Society, New York, 1982.
- 3. C. J. Mogab, A. C. Adams, and D. L. Flamm, J. Appl. Phys. 49, 3796 (1978).
- 4. R. D'Agostino, F. Cramarossa, S. De Benedictis, and G. Ferraro, J. Appl. Phys. 52, 1259 (1981).
- R. H. Bruce, J. Appl. Phys. 52, 7064 (1981).
 C. Wild and P. Koidl, Appl. Phys. Lett. 54, 505 (1989).
- 7. J. W. Coburn and H. F. Winters, J. Appl. Phys. 50, 3189
- 8. H. F. Winters, J. W. Coburn, and T. J. Chuang, J. Vac. Sci. Technol. B 1, 469 (1983).
- 9. J. L. Mauer, J. S. Logan, L. B. Zielinski, and G. C. Schwartz, J. Vac. Sci. Technol. 15, 1734 (1978).
- 10. T. J. Tu, T. J. Chuang, and H. F. Winters, Phys. Rev. B 23, 823 (1981).
- 11. J. A. Yarmoff and F. R. McFeely, Surf. Sci. 184, 389 (1987).
- 12. H. F. Winters and J. W. Coburn, Mater. Res. Soc. Symp. Proc. 38, 189 (1985).
- 13. R. A. Haring, A. Haring, F. W. Saris, and A. E. de Vries, Appl. Phys. Lett. 41, 174 (1982).

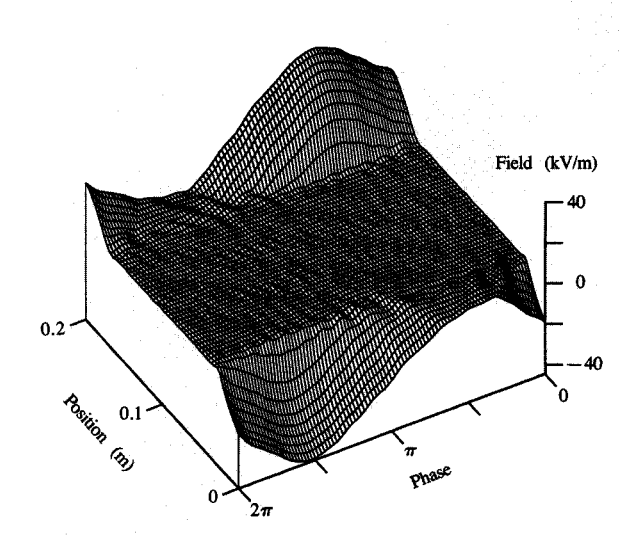


Figure 14

Results of particle-in-cell simulation of the plasma in a symmetric parallel-plate rf reactor, assuming a frequency of 10 MHz, a pressure of 20 mtorr, and $V_{rf} = 1 \text{ kV}$. The evolution of the electric field in the space between the two electrodes is shown as a function of time. Note that there is no electric field in the bulk of the discharge and that all the field variations are located in the sheath regions. From [93], reproduced with permission. © 1990 IEEE.

- 14. A. W. Kolfschoten, R. A. Haring, A. Haring, and A. E. de Vries, J. Appl. Phys. 55, 3813 (1984).
- 15. G. C. Schwartz and P. M. Schaible, J. Vac. Sci. Technol. 16, 410 (1979).
- 16. M. Nakamura, K. Iizuka, and H. Yano, Suppl. a la Revue "Le Vide, les Couches Minces" **246**, 74 (1989).
- 17. T. D. Bestwick and G. S. Oehrlein, J. Vac. Sci. Technol. A 8, 1696 (1990).
- 18. G. C. Schwartz and P. M. Schaible, J. Electrochem. Soc. 130, 1898 (1983).
- 19. H. F. Winters and D. Haarer, Phys. Rev. B 36, 6613
- 20. E. A. Ogryzlo, D. E. Ibbotson, D. L. Flamm, and J. A. Mucha, J. Appl. Phys. 67, 3115 (1990).
- 21. G. K. Herb, D. J. Rieger, and K. Shields, Solid State Technol. 30, 109 (1987).
- 22. R. N. Carlile, V. C. Liang, O. A. Palusinski, and M. M. Smadi, J. Electrochem. Soc. 135, 2058 (1988).
- 23. M. Sato and Y. Arita, J. Electrochem. Soc. 134, 2856 (1987).
- 24. G. S. Oehrlein, J. F. Rembetski, and E. H. Payne, J. Vac. Sci. Technol. B 8, 1199 (1990).
- 25. J. F. O'Hanlon, A User's Guide to Vacuum Technology, John Wiley, New York, 1980.
- 26. D. L. Smith and R. H. Bruce, J. Electrochem. Soc. 129, 2045 (1982).
- 27. D. L. Smith and P. G. Saviano, J. Vac. Sci. Technol. 21, 768 (1982).
- 28. F. H. Sanders, A. W. Kolfschoten, J. Dieleman, R. A. Haring, A. Haring, and A. E. de Vries, J. Vac. Sci. Technol. A 2, 487 (1984).

- 29. J. Dieleman, F. H. Sanders, A. W. Kolfschoten, P. C. Zalm, A. E. de Vries, and A. Haring, J. Vac. Sci. Technol. B 3, 1384 (1985).
- 30. P. E. Clarke, D. Field, and D. F. Klemperer, J. Appl. Phys. 67, 1525 (1990).
- 31. G. S. Oehrlein, K. K. Chan, M. A. Jaso, and G. W. Rubloff, J. Vac. Sci. Technol. A 7, 1030 (1989).
- 32. M. Sekine, T. Arikado, H. Okano, and Y. Horiike, in Proceedings of the Eighth Symposium on Dry Process, Jun-ichi Nishizawa, Ed., Institute of Electrical Engineering, Tokyo, 1986, p. 42. 33. T. Arikado, K. Horioka, M. Sekine, H. Okano, and Y.
- Horiike, Jpn. J. Appl. Phys. 27, 95 (1988).
- 34. M. Engelhardt and S. Schwarzl, in Proceedings of the Ninth Symposium on Dry Process, Jun-ichi Nishizawa, M. Hirose, Y. Horiike, and K. Suto, Eds., The Electrochemical Society, Pennington, NJ, 1988, p. 48.
- 35. M. Nakamura, K. Iizuka, and H. Yano, Jpn. J. Appl. Phys. 28, 2142 (1989).
- 36. K. Hirobe, K. Kawamura, and K. Nojiri, J. Vac. Sci. Technol. B 5, 594 (1987).
- 37. T. P. Chow, P. A. Maciel, and G. M. Fanelli, J. Electrochem. Soc. 134, 1281 (1987).
- 38. G. S. Oehrlein, R. G. Schad, and M. A. Jaso, Surf. Interf. Anal. 8, 243 (1986).
- 39. I. W. Rangelow, P. Thoren, K. Masseli, R. Kassing, M. Engelhardt, and S. Schwarzl, Microelectron. Eng. 5, 387
- 40. D. J. Thomas, P. Southworth, M. C. Flowers, and R. Greef, J. Vac. Sci. Technol. B 7, 1325 (1989).
- 41. S. Tachi, K. Tsujimoto, and S. Okudaira, Appl. Phys. Lett. 52, 616 (1988).
- 42. D. Chin, S. H. Dhong, and G. J. Long, J. Electrochem. Soc. 132, 1705 (1985)
- 43. C. J. Mogab and H. J. Levinstein, J. Vac. Sci. Technol. **17**, 721 (1980).
- 44. G. S. Selwyn, J. Appl. Phys. 60, 2771 (1986).
 45. Y. H. Lee and Z. H. Zhou, in Proceedings of the Eighth Symposium on Plasma Processing, G. S. Mathad and D. W. Hess, Eds., The Electrochemical Society, Pennington, NJ, 1990, p. 34.
- 46. D. J. Economou and R. C. Alkire, J. Electrochem. Soc. 135, 941 (1988).
- 47. J. W. Coburn and H. F. Winters, Appl. Phys. Lett. 55, 2730 (1989).
- 48. H. C. Jones, R. Bennett, and J. Singh, in Proceedings of the Eighth Symposium on Plasma Processing, G. S. Mathad and D. W. Hess, Eds., The Electrochemical Society, Pennington, NJ, 1990, p. 45.
- 49. K. Nojiri, E. Iguchi, K. Kawamura, and K. Kadota, in Extended Abstracts of the 21st Conference on Solid State Devices and Materials, Business Center for the Academic Society of Japan, Tokyo, 1989, p. 153
- 50. B. E. Thompson, H. H. Sawin, and D. A. Fisher, J. Appl. Phys. 63, 2241 (1988).
- 51. R. A. Heinecke, Solid State Electron. 18, 1146 (1975).
- 52. L. M. Ephrath, J. Electrochem. Soc. 126, 1419 (1979).
- 53. H. W. Lehmann and R. Widmer, J. Vac. Sci. Technol. 15,
- 54. G. S. Oehrlein and H. L. Williams, J. Appl. Phys. 62, 662 (1987); G. S. Oehrlein, S. W. Robey, and M. A. Jaso, Mater. Res. Symp. Proc. 98, 229 (1987).
- 55. G. S. Oehrlein, S. W. Robey, J. L. Lindström, K. K. Chan, M. A. Jaso, and G. J. Scilla, J. Electrochem. Soc. 136, 2051 (1989).
- 56. M. M. Millard and E. Kay, J. Electrochem. Soc. 129, 160 (1982).
- 57. P. J. Hargis, Jr. and M. J. Kushner, Appl. Phys. Lett. 40, 779 (1982).
- 58. G. S. Oehrlein, Mater. Sci. Eng. B 4, 441 (1989).
- 59. R. G. Frieser, F. J. Montillo, N. B. Zingerman, W. K. Chu, and S. R. Mader, J. Electrochem. Soc. 130, 2237 (1983).

- 60. D. J. Vitkavage and T. M. Mayer, J. Vac. Sci. Technol. B 4, 1283 (1986).
- 61. G. S. Oehrlein, R. M. Tromp, J. C. Tsang, Y. H. Lee, and E. J. Petrillo, J. Electrochem. Soc. 132, 1441 (1985).
- 62. J. C. Mikkelsen, Jr. and D. Wu, Appl. Phys. Lett. 49, 103 (1986).
- 63. C. Cardinaud, A. Rhounna, G. Turban, and B. Grolleau, J. Electrochem. Soc. 135, 1472 (1988).
- 64. Y. Ozaki and K. Ikuta, Jpn. J. Appl. Phys. 23, 1526
- 65. M. Ostling, C. S. Petersson, H. Norstrom, R. Buchta, and H. Blom, J. Vac. Sci. Technol. B 5, 586 (1987).
- 66. G. S. Oehrlein and Y. H. Lee, J. Vac. Sci. Technol. A 5, 1585 (1987).
- 67. G. J. Coyle and G. S. Oehrlein, Appl. Phys. Lett. 47, 604
- 68. H. Cerva, E. Mohr, and H. Oppolzer, J. Vac. Sci. Technol. B 5, 590 (1987).
- 69. S. J. Jeng and G. S. Oehrlein, Appl. Phys. Lett. 50, 1912
- 70. G. S. Selwyn, J. Singh, and R. S. Bennett, J. Vac. Sci. Technol. A 7, 2758 (1989)
- 71. G. S. Selwyn, J. E. Heidenreich, and K. L. Haller, Appl. Phys. Lett. 57, 1876 (1990).
- 72. J. A. O'Neill, J. Singh, and G. G. Gifford, J. Vac. Sci. Technol. A 8, 1716 (1990).
- 73. G. M. Jellum and D. B. Graves, J. Appl. Phys. 67, 6490 (1990).
- 74. A. von Engel, Electric Plasmas: Their Nature and Uses, Taylor & Francis Inc., New York, 1983.
- 75. J. A. Thornton, J. Vac. Sci. Technol. 15, 171 (1978).
- 76. M. Engelhardt, Solid State Technol. 33, 151 (1990).
- 77. S. V. Nguyen, D. Dobuzinsky, S. Stiffler, and G. Chrisman, in Proceedings of the Eighth Symposium on Plasma Processing, G. S. Mathad and D. W. Hess, Eds. The Electrochemical Society, Pennington, NJ, 1990, p. 491.
- 78. K. Suzuki, S. Okudaira, N. Sakudo, and I. Kanomata, Jpn. J. Appl. Phys. 16, 1979 (1977).
- 79. S. Matsuo, Appl. Phys. Lett. 36, 768 (1980).
- 80. A. S. Yapsir, G. S. Oehrlein, F. Wiltshire, and J. C. Tsang, Appl. Phys. Lett. 57, 590 (1990).
- 81. R. W. Boswell and R. K. Porteous, J. Appl. Phys. 62, 3123 (1987).
- 82. G. C. Schwartz, in Proceedings of the Fifth Symposium on Plasma Processing, G. S. Mathad, G. C. Schwartz, and G. Smolinsky, Eds., The Electrochemical Society, Pennington, NJ, 1985, p. 26.
- 83. P. Banks, W. Pilz, I. Hussla, G. Lorenz, and G. Castrischer, Proc. SPIE 1037, 35 (1989).
- 84. D. Angell and G. S. Oehrlein, in Proceedings of the Eighth Symposium on Plasma Processing, G. S. Mathad and D. W. Hess, Eds., The Electrochemical Society, Pennington, NJ, 1990, p. 171.
- 85. D. B. Graves and K. F. Jensen, IEEE Trans. Plasma Sci. PS-14, 78 (1986).
- 86. J. H. Keller and W. B. Pennebaker, IBM J. Res. Develop. 23, 3 (1979).
- 87. M. A. Lieberman, IEEE Trans. Plasma Sci. 16, 638 (1988).
- 88. G. R. Misium, A. J. Lichtenberg, and M. A. Lieberman, J. Vac. Sci. Technol. A 7, 1007 (1989).
- 89. J. P. Boeuf, J. Appl. Phys. 63, 1342 (1988).
- 90. A. D. Richards and H. H. Sawin, J. Appl. Phys. 62, 799
- 91. E. Gogolides, J. Nicolai, and H. H. Sawin, J. Vac. Sci. Technol. A 7, 1001 (1989).
- 92. M. J. Kushner, IEEE Trans. Plasma Sci. PS-14, 188 (1986).
- 93. D. Vender and R. R. Boswell, IEEE Trans. Plasma Sci. 18, 725 (1990).
- J. I. Ulacia and J. P. McVittie, J. Appl. Phys. 65, 1484 (1989).

- J. Pelka, M. Weiss, W. Hoppe, and D. Mewes, J. Vac. Sci. Technol. B 7, 1483 (1989).
- H. Feil, J. van Zwol, S. T. de Zwart, J. Dieleman, and B. J. Garrison, *Phys. Rev. B* 43, 13695 (1991).
- 97. J. A. Bondur, J. Vac. Sci. Technol. 13, 1023 (1976).

Received October 15, 1991; accepted for publication February 26, 1992

Gottlieb S. Oehrlein IBM Research Division, Thomas J. Watson Research Center, P.O. Box 218, Yorktown Heights, New York 10598 (OEHR at YKTVMZ, oehr@watson.ibm.com). Dr. Oehrlein is a Research Staff Member in the Silicon Technology Department at the Thomas J. Watson Research Center. He received a Vordiplom degree in physics from Wuerzburg University in West Germany in 1976, and M.S. and Ph.D. degrees in physics from the State University of New York at Albany in 1978 and 1981, respectively. He subsequently joined IBM at the Thomas J. Watson Research Center, where he has worked on exploratory materials and plasma-based processes. In 1989 Dr. Oehrlein received an IBM Outstanding Technical Achievement Award for his work on reactive ion etching. Currently his research interests pertain to the fundamental aspects of plasma etching, plasma-enhanced chemical vapor deposition, and the integration of plasma-based processes in vacuum cluster tools.

John F. Rembetski IBM Technology Products, Burlington facility, Essex Junction, Vermont 05452 (USSEM7B6 at IBMMAIL, john_rembetski@sematech.org). Mr. Rembetski is a Staff Engineer in the Plasma Process Development Department in the Advanced Technology organization at the IBM Essex Junction facility. He joined IBM in 1985 after receiving his B.S. and M.S. degrees in chemical engineering from Clarkson University. His M.S. thesis work was carried out in connection with plasma-related work at the IBM Endicott facility. Mr. Rembetski has received several IBM Invention Achievement Awards for patents and disclosures. He is currently on assignment at Sematech in Austin, Texas, working on the characterization of plasma etching damage and the development of high-density plasma etching processes.